MRS Communications

Research Letter

On the 3D printability of one-part moisture-curable polyurethanes via direct ink writing (DIW)

Carla Joyce C. Nocheseda, Department of Chemical and Biomolecular Engineering, Department of Materials Science and Engineering, and Department of Electrical Engineering and Computer Science, and The University of Tennessee, Knoxville, TN, USA

G. M. Fazley Elahee, Department of Macromolecular Sciences and Engineering, Case Western Reserve University, Cleveland, OH, USA; Novagard Solutions, Cleveland, OH 44114, USA

Marielle Francesca A. Santos, Department of Chemical and Biomolecular Engineering, Department of Materials Science and Engineering, and Department of Electrical Engineering and Computer Science, and The University of Tennessee, Knoxville, TN, USA

Xiang Cheng, Department of Macromolecular Sciences and Engineering, Case Western Reserve University, Cleveland, OH, USA

Alejandro H. Espera Jr., Department of Chemical and Biomolecular Engineering, Department of Materials Science and Engineering, and Department of Electrical Engineering and Computer Science, and The University of Tennessee, Knoxville, TN, USA

Rigoberto C. Advincula[ID], Department of Chemical and Biomolecular Engineering, Department of Materials Science and Engineering, and Department of Electrical Engineering and Computer Science, and The University of Tennessee, Knoxville, TN, USA; Department of Macromolecular Sciences and Engineering, Case Western Reserve University, Cleveland, OH, USA; Center for Nanophase Materials and Sciences, Oak Ridge National Laboratory, Oak Ridge, TN 37830, USA

Address all correspondence to Rigoberto C. Advincula at **radvincu@utk.edu**

Abstract

Direct ink writing (DIW) is an ambient temperature additive manufacturing (AM) method that accommodates many possible ink materials. Here, we demonstrate using a moisture-curable commercially available polyurethane (PU) sealant as an alternative ink for DIW. We discussed the fundamentals of PU chemistry and determined the best 3D printing parameters. Studies on rheological, thermogravimetric, spectroscopic characterization, and initial finite element analyses (FEA) showed properties expected from a performance sealant with high elongation and low modulus of a 3D-printed object. This affirms the flexibility of the DIW technique as an accessible AM method amenable for future materials development from commercial model formulations.

Introduction

Additive manufacturing (AM) or 3D printing offers unavailable fabrication techniques using conventional manufacturing routes with customized designs and complex geometric shapes and sizes.[1,2] Conventional casting and injection molding techniques can be challenging when parts have hollow interiors and internal channels. In 3D printing, there is no need to make complex molds with complex components that add cost.[3,4] Many industries have adopted AM as a manufacturing method for limited parts or prototype production.[5–8]

The most common AM technique is the fused filament fabrication technique (FFF) or more popularly known as fused deposition modeling (FDM). It simply involves melting a polymer in filament form in a temperature-controlled nozzle head. The nozzle moves and precisely extrudes the melt polymer until the desired shape or geometry is achieved to produce a layer-by-layer polymer structure.

3D printing is typically associated with engineering thermoplastics as it is the most common feedstock for commercially available 3D printers. However, interest in exploring materials with interesting functional properties is becoming popular.[9,10] Direct ink writing or (DIW) is another AM technique similar to FFF and FDM but operates at an ambient temperature. Commonly used in the 3D printing of scaffolds for cell culturing in tissue engineering, it is now gaining popularity due to its ability to accommodate almost any possible viscous or slurry material as feedstock.[8]

Lewis et al.[11] described the direct-write mechanism as similar to a CNC movement where a translation stage moves a nozzle head containing an ink material to deposit and create a controlled architecture. They further classified DIW into two (2) droplet- or filament-based approaches. The filament-based approach to direct writing includes robocasting, FDM and related methods, and freeform extrusion fabrication (EFF). In both approaches, ink is continuously extruded through a fine nozzle to create a filament. Both robocasting and FFF are best for shear-thinning materials.

Under filament-based DIW, ink delivery can be described in two ways[11]—the constant-displacement and constant-pressure extrusion. Using a single or multiple nozzle system can give continuous filament in both ways. The nozzle diameter, ink rheology, and printing speed determine the filament diameter. In constant-displacement printing, a plunger is applied to the

ink container creating a uniform flow of ink at a pressure to achieve the desired flow.

While in constant-pressure printing, a uniform pressure is applied to the ink container. This approach is, however, less common.

Colloidal gels are the best materials for DIW of complex 3D structures.[12] Their viscoelastic properties allow easy flow through nozzles and produce filaments with rigid shapes. Two essential criteria must be considered when designing or using inks suitable for DIW. First, it must have a controlled viscoelastic response to flow through the nozzle and immediately becomes rigid to retain shape and features; second, it must have minimum drying-induced shrinkage after printing to resist better compressive stresses arising from capillary tension.

Sealants are readily available commercial materials that are used to seal or restrict fluids and other substances from passing through the mechanical joints and surfaces of a building.[13] It blocks dust, acoustics, air leakage, heat, and insects. Still, the primary purpose of this construction material remains to fill the gaps between surfaces where concrete cannot be used. Sealants come in a wide variety of options and their characteristics differ. Polyurethane (PU)-based sealants feature the following advantages: textured appearance that blends well with different masonry substrates; flexibility, paintable, moveable, and adheres to various surfaces providing a leak-proof bonding. There should be differences in properties between sealants and adhesives regarding strength and elongation, but suppliers lack consistency about this differentiation.

Crescentini et al.[14] described PUs as typically found in flexible and rigid foams, thermoplastics, thermosets, adhesives, and sealants due to their polymeric versatility. Originally developed as a replacement for rubber in the 1930s, it is now a common material that has found itself helpful in insulation to mattresses, varnishes, couches, paints, adhesives, and elastic fibers.[15] It is relatively easy to alter in many different ways. PUs are common materials with high-performance sealants with high elongation and low modulus and are suitable for commercial buildings and construction for exterior and interior sealing. PUs have properties imparted to elastomeric sealants, for example, prepared from the reaction of hydroxy-functional components with isocyanate-functional components.

Our current work uses a commercially available one-part fast-curing PU sealant composition. The isocyanate (NCO)-terminated urethane quasi-prepolymers react in the presence of moisture resulting in cured prepolymers.[16] Solid and flexible seals formed under average temperature and moisture conditions when one-part sealant compositions react. Figure 1(a) represents their significant structural segment. PUs can be customizable depending on their applications.[14] Additives that enhance desired properties may include but are not limited to cross-linkers, fillers, etc.[17]

This paper describes the chemistry and characterization that dictates the properties of PU as a material and its 3D printability. This is valuable in the printing process before a viscous polymer is formed. Although readily and commercially available, PU-based sealants are not commonly used as ink for 3D printers. Our work aims to look closely at the chemistry and composition of readily available commercial PUs and how it correlates as an alternative ink in DIW. By understanding the chemistry, rheology, and printing parameters, we set the groundwork for future work involving further improving PU formulations and their properties in 3D printing. Additionally, we report analyzing the PU sealant's mechanical and electrical performance as 3D-printed structures.

Experimental section
Materials
A formulated PU sealant, Loctite® PL® Concrete Crack, and Masonry Sealant were used. The manufacturer's website[18] described it as a high-quality one-component, texturized, moisture-curing gun-grade sealant specifically formed as weatherproof seals. Its textured appearance blends well with masonry substrates exhibiting limestone or gray color. Once cured, it does not sag and remains elastic and flexible to expand and contract. It does not need any primer or quickly degrade from weather, stress, or movement. Technical specification on the manufacturer's website[18] shows that its uncured base is formaldehyde and asbestos-free PU. It contains mineral spirits and toluene di-isocyanate (TDI). Nothing further about its chemistry is provided beyond the MSDS data.

3D printing
As with any 3D printing technique, printing uses a computer-aided design (CAD) object.[19] A standard tessellation language (STL) format was obtained that a 3D printer could read. The PU sealant was contained in a 10-mL syringe and placed into the extrusion head device in the 3D printer (Hyrel 3D, Engine SR model)[20] guided by CNC movement, see the schematic image in Fig. 1(b). The syringe can move in the *XYZ* directions as dictated by the geometrical design down to the material-level design from the stl file. Dispensing materials using nozzles into 3D structures layer by layer is well known.[21] The ink material was printed onto acetate film placed on the printing platform for easy removal after printing. Luer locks standard nozzle sizes from 250 μm (inside diameter, gauge 25) to 810 μm (inside diameter, gauge 18) was used to 3D print the ink. At least a 1-mm distance is maintained between the build platform and the nozzle tip performed before printing, a standard procedure set with the 3D printer. The printing parameters are summarized in Fig. 1(c). After printing, the printed structures were allowed to dry at an ambient temperature for 24 h to 3 days. An extrusion rate of 15–20 mL/h and a nozzle moving rate of 10–15 mm/s were used in the 3D printing process.

Methodology and instrumentation
Rheology
Rheological characterization was conducted on a Discovery HR20 rotational parallel plate rheometer (TA Instruments, New
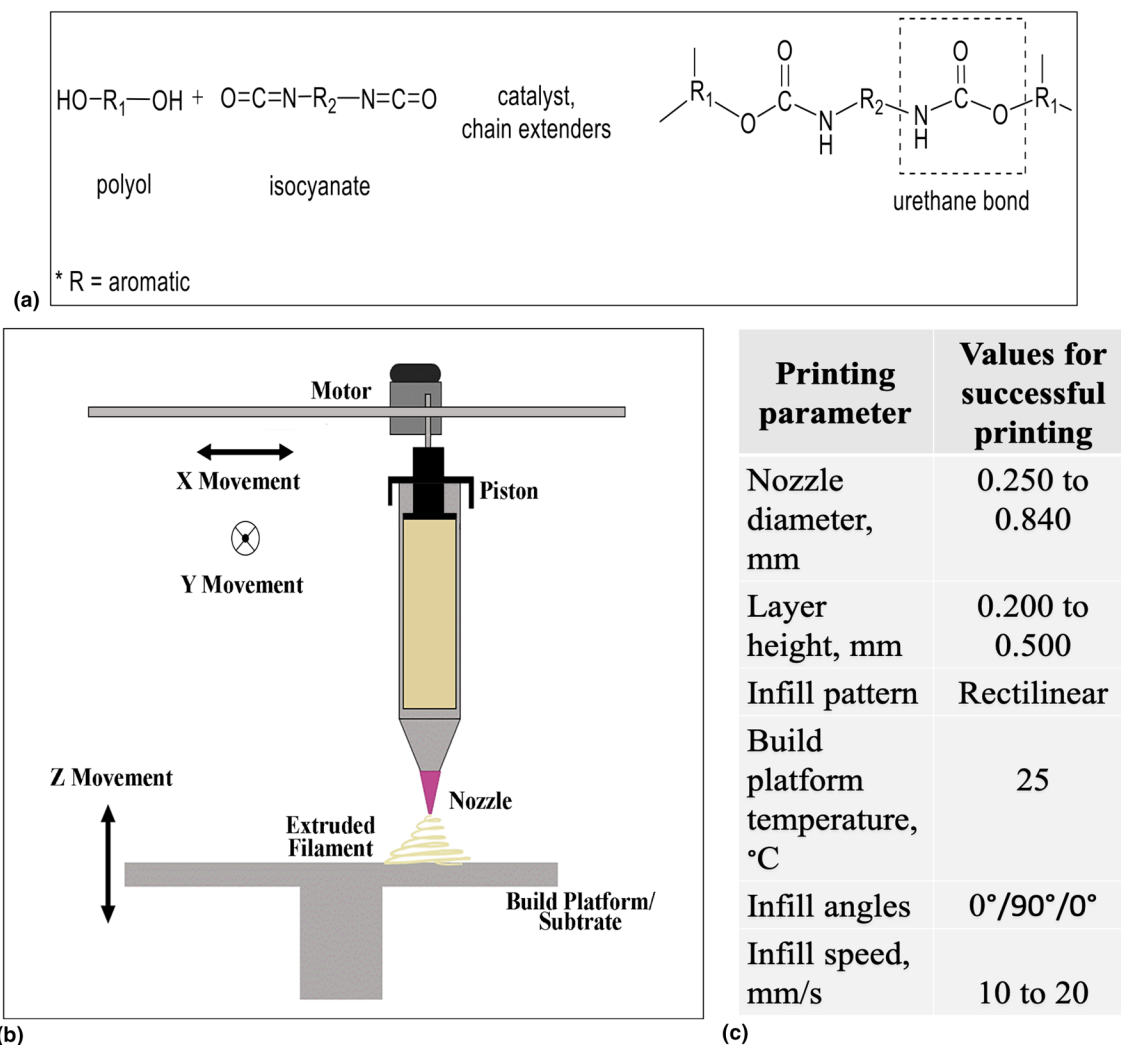
Figure 1. (a) Basic polyurethane reaction scheme between polyol and isocyanates to form a urethane group, (b) schematic image showing the DIW of commercially available polyurethane sealant, and (c) DIW parameters showing the range of values can be used to successfully 3D print PU sealant.

Castle, DE, USA) with a force rebalance transducer, second-generation magnetic bearing, and an accurate position sensor in a single head with 25-mm upper and lower parallel plate geometry associated with the Peltier plate base that was held at 25°C for all steady-state shear deformation rheology tests in this study. The plate gap was set to 1 mm, with a 2-min conditioning time before the measurements. Frequency sweeps up to 100 Hz were applied to determine the linear viscoelastic region and the shear thinning and yield stress. Dynamic oscillatory sweeps are conducted at 1 Hz under controlled stress.

Scanning electron microscope with EDS

Scanning electron microscopy–energy-dispersive X-ray (SEM–EDX) characterization was performed on 3D-printed cured samples using a JEOL 6010 Plus. Each analyte was placed on an aluminum sample holder using carbon tape for holding.

Fourier transform infrared spectroscopy (FTIR)

Fourier transform infrared spectroscopy (FTIR) measurement was performed on a 3D-printed cured sample using a Cary 600 Series FTIR spectrometer (Agilent Technologies). Specifically, 32 scans were carried out in the 400–4000 cm^{-1} range with a resolution of 0.5 cm^{-1}.

Thermogravimetric analysis (TGA)

TGA characterizations were carried out in a TA Instrument SDT Q600 utilizing platinum crucibles, with a heating rate of 10°C/min from room temperature up to 900°C under a flux of ultrahigh-purity nitrogen (100 mL/min). The analysis was performed using approximately 3.5 mg of 3D-printed cured samples.

Pyrolysis-GC/MS and evolved gas analysis (EGA)

EGA experiment was conducted using GC–MS (Agilent 5973, Quantum Analytics) equipped with a Multi-Shot Pyrolyzer (EGA/PY-3030D, Frontier Lab). A short metal column (Ultra ALLOY—DTM; length 2.5 m, I.D. 0.15 mm, O.D. 0.25 mm, Frontier lab) was used.

About 0.2 mg of the testing sample was placed into a sample cup. Then the sample cup was put into a preheated Pyrolyzer at 100°C. The Pyrolyzer was heated at 20°C/min until 700°C, and the evolved gas was directly injected into the short column under a helium flow (1 mL/min). The GC oven temperature was initially set at 40°C and heated to 300°C. The interface between GC/MS and Pyrolyzer was maintained at 200°C. All detected peaks were determined according to the Frontier Labs library and the NIST library.

Finally, the 3D-printed parts were characterized and evaluated for properties, including curing time, density, dielectric constant, dissipation factor, breakdown voltage, volume resistivity, durometer hardness, compression deflection, tensile strength, thermal conductivity, thermal diffusivity, and specific heat. See Supplementary Information (SI) for details of measurement methods and results.

Results and discussion
Isocyanate NCO-terminated quasi-prepolymers

PU compositions have been used as sealants due to their many desirable properties, such as high bond strength, flexibility, and fatigue resistance. PU has disadvantages, including slow curing speed and low bonding strength, due to foaming by carbon dioxide.[15] Its properties depend on the cross-linking reaction designed to occur once the sealant is applied.[16] Unsurprisingly, the interest in studying this one-component, solvent-free urethane sealant based on isocyanate-terminated PUs is still increasing.

This sealant is generally obtained by reacting moisture with isocyanate NCO-terminated quasi-prepolymers. Excess di-isocyanates and polyols are reacted, producing a prepolymer with free isocyanate functionality.[22,23] These free isocyanates are highly reactive and can be toxic.[16] The isocyanate group is di-isocyanates that may have two or more two –NCO groups per molecule. It has the cumulated double-bond sequence represented by R–N=C=O, see Fig. S1(a), wherein the more electropositive character of the carbon (C) atom dictates the reactivity of isocyanate.[13] The R here is an aromatic group since, as per the manufacturer's website,[17] aromatic TDI is used. An aromatic group usually has a negative charge, see Fig. S1(a) making the aromatic isocyanates more reactive. Polyols are substances that have a plurality of hydroxyl groups. Polyester polyol (PEP) consists of ester and hydroxyl groups in one backbone. An excellent example of naturally occurring PEP is castor oil. On the manufacturer's website,[17] the PU sealant used here is said to contain mineral spirits. The properties of the PU depend on the degree of cross-linking and molecular weight of the starting PEP. Short-chained PEP gives PU good flexibility and low chemical resistance, while high-molecular weight long-chain polyols yield flexible PU. PEPs are susceptible to hydrolysis, which may lessen their mechanical properties. As such, adding metal salts or small amounts of carbodiimides is common. The free isocyanates from the reaction of isocyanates and polyols are reacted with air and moisture forming urea groups, see Fig. S1(b). Carbamic acid intermediate is formed and dissociates to yield carbon dioxide and an amine which further reacts with other NCO groups to form urea linkage.

Additives may be added to control and modify the reaction conditions of PU. These include catalysts, chain extenders, cross-linkers, and fillers. Typical catalysts include amine-based 1, 4-di-aza-bicyclo-(2, 2, 2)-octane (DABCO), or tin-based di-butyl-tindi-laurate (DBTDL).[24] It must be noted that many of the proprietary iterations of PU or poly(urethane urea) (PUU) compositions exist and are composed of a variety of different combinations and ratios of catalyst, fillers, and compounds that allow the improvement of desired properties such as excellent adhesion to various surfaces.

When used as ink for DIW, isocyanate NCO-terminated prepolymer starts to cure or polymerize when exposed to atmospheric or added moisture forming urea groups. The reaction creates a carbamic acid intermediate dissociating to carbon dioxide that further reacts with an amine and other NCO groups to form urea linkages, see Fig. S1(b). Da Silva et al.[16] described the curing mechanism between the low-molecular weight liquid PUU solid transforming to a high-molecular weight solid as having similar properties to that of a thermoset. The partial mutual insolubility of soft and hard domains PUU results in a two-phase morphology that, although thermodynamically incompatible, creates microphase separation between hard and soft segments. PUUs' properties strongly depend on the balance between microphase separation and mixing. The interaction between soft and hard segments changes as the curing proceeds, depending on the prepolymer composition.

Rheology

For the printing of PU, rheological measurements are required to know the cross-linking time when the soft material extruded from the nozzle can transform into a rigid shape supporting the succeeding layer. PU must have high storage modulus (G'), shear-thinning behavior, high yield stress (τ_y), and fast elastic recovery to direct ink-write complex shapes. Filaments do not sag if storage modulus G' is high. High yield stress prevents distortion of the printed structure due to capillary forces. By measuring the crossover point where the storage modulus, G' and loss modulus, G'' curves intersect under constant amplitude, we can estimate the region or range of stress values that would allow the ink to exhibit clear viscoelastic behavior during printing ($G' > G''$) and critical shear strain ($G' < G''$). It has shear-thinning behavior and quick elastic recovery that
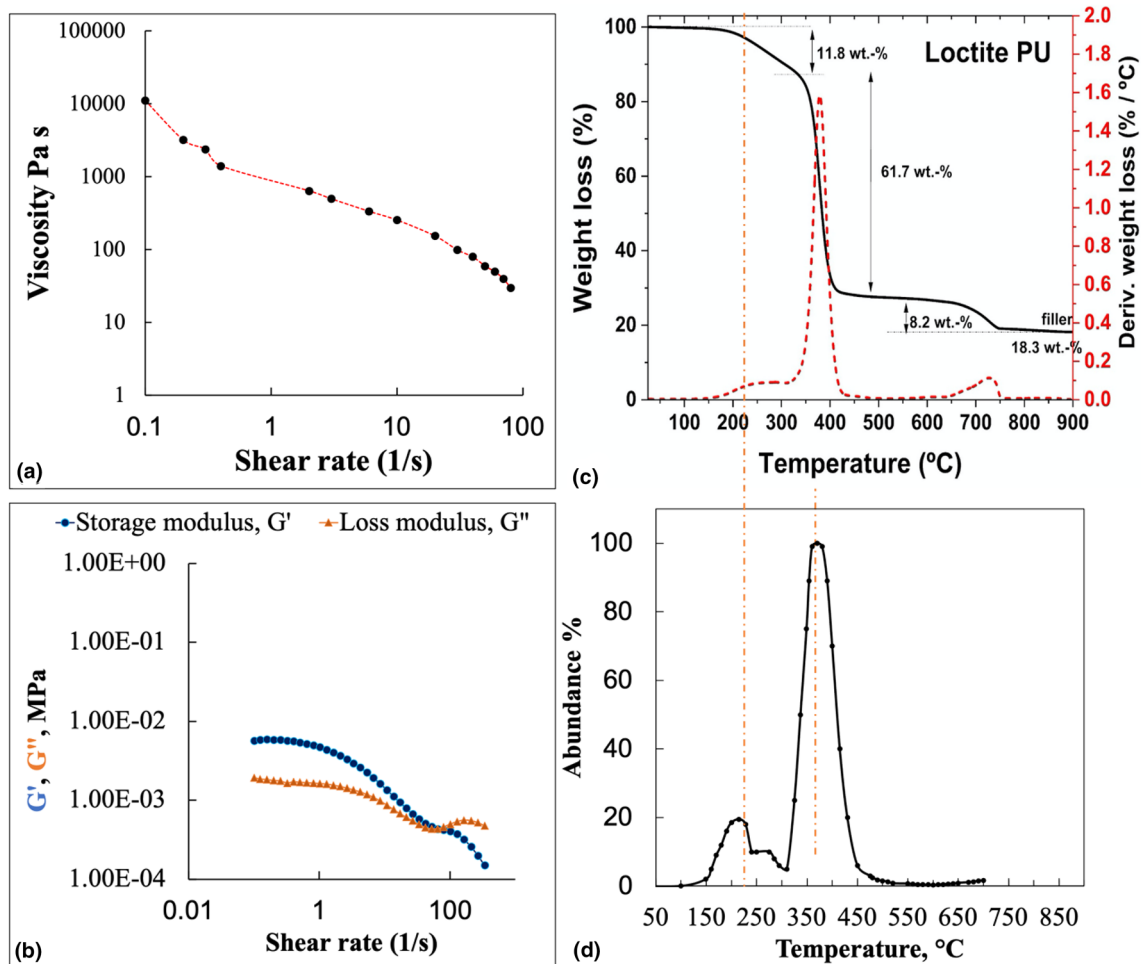
Figure 2. (a) Viscosity over shear rate curve of polyurethane sealant and (b) crossover point where the storage modulus, *G'* and loss modulus, *G"* curves intersect under constant amplitude; (c) TGA and (d) EGA thermograms of polyurethane sealant.

significantly influence the extrusion and cross-linking of the PU during and shortly after the extrusion of the filaments.

Rheological measurements are presented for a PU sealant, as shown in Fig. 2(a)–(b). Viscosity over the shear rate, Fig. 2(a) shows a downward decreasing curve that indicates the shear-thinning behavior of PU that is critical for successful DIW. It is noted here that the shear rate has to be very small as edge instabilities were observed during measurement if the shear rate value is increased. Oscillatory measurement, Fig. 2(b) indicates that PU shows a viscoelastic behavior, showing elastic behavior at low strains ($G' > G''$) and plasticity above a critical shear strain ($G' < G''$). The storage modulus (G') of 8 kPa obtained is sufficient to print rigid structures with no sagging of filaments.

Thermogravimetric analysis (TGA) and evolved gas analysis (EGA)

TGA and EGA were conducted to determine the thermal stability of PU sealant. Figure 2(c)–(d) shows the TGA and EGA spectra of the PU sealant from 30 to 900°C and from 30 to 700°C, respectively. Figure 2(c)–(d) shows the TGA and EGA

spectra aligned to show the correlation between EGA and TGA. This is because the EGA technique is very similar to the TGA; the EGA spectrum is derived from a gas chromatography–mass spectroscopy (GC–MS) that uses a pyrolyzer to control the temperature applied to a sample in a sample cup. The gaseous components will evolve at different temperatures and pass through the GC column and then the MS detector. The intensity of the MS signal (%abundance) will be accumulated and shown on *Y*-axis, as seen in Fig. 2(d).

The PU sealant has three degradation slopes observed from the TGA spectrum, Fig. 2(c). The first TGA degradation slope did not occur until 100°C to 350°C with a weight loss of 11.8 wt%. This slope refers to the start of the depolymerization of the urethane since PUs are known to be relatively thermally unstable materials.[25] This slope relates to splitting the urethane bond into secondary amine and carbon dioxide.[25] PU dissociates into its starting component: isocyanates and polyol. The isocyanates are then dimerized, volatilizing small molecule compounds, such as carbon oxides and amines, to form carbodiimides, resulting in the onset temperature of the first

degradation peak estimated at 220°C. It aligns to the apex of the first EGA peak, see Fig. 2(d). The third degradation peak is about 730°C at 8.2 weight loss, resulting from carbodiimide reaction with alcohol. However, this temperature cannot be verified due to the limitation in the temperature range of EGA.

The TGA and EGA temperatures are comparable, with a 5% difference. A significant amount of 20-wt% ash is left at 900°C, as shown in Fig. 2(d). We can attribute this to the fact that it is prevalent for sealants to have many different kinds of additives that may include plasticizers, fillers, and thixotropes to change its physical properties.

Scanning electron microscopy and EDS

Using SEM and EDX spectroscopy, see Fig. 3(c)–(e), elemental analysis of the composition of the PU sealant is conducted to know what could comprise the 20% ash or char observed in the TGA curve.

It shows scanning electron microscope images for PU sealant samples using secondary electron imaging at the cross-section, Fig. 3(c)–(d). It offers excellent compatibility and wettability between the fillers and the PU sealant matrix. Figure 3(e) shows the EDS spectra, including elemental composition results. The elements detected are composed mainly of C and O, compatible with PU. The significant amount of C means carbon black is added. There are traces of Ti and Ca, as many PU sealants typically contain calcium carbonate and titanium dioxide fillers. Al is detected, maybe due to some presence of aluminum oxide. Fillers are commonly added to improve leveling and prohibit sagging.

Fourier transform infrared spectroscopy (FTIR)

FTIR spectra of PU sealant are shown in Fig. 4(a). The presence of N–H group at 3452 cm^{-1}, carbonyl groups at 1733 cm^{-1} (C=O stretching), 1100 cm^{-1} (C–O stretching), and peaks at 3000 cm^{-1} and 2875 cm^{-1} CH anti-symmetric and symmetric stretching, respectively, are all observed. Stretching of carbonate at the band of 1350 to 1400 cm^{-1} is also detected. No band for terminal NCO groups is detected. These unique bands highlight the common carbamate unit. We can relate this FTIR result to common knowledge that PUs are made of flexible chains lined by aromatic segments. The hydrogen bonds between polar groups, mainly among N–H groups (electron acceptors) and carbonyl groups (electron donors), determine the PU's character, which is all observed in the FTIR spectra.

Here, we see very few peaks for C=O and N=H that are responsible for hydrogen bonds. These hydrogen bonds in typical PU are responsible for additional strength in the polymer matrix; sealant reformation during elongation; and bond with a plasticizer with a C=O or carbonyl group in its chain structure.

Gas chromatography–mass spectroscopy (GC–MS)

The mass spectra for PU are shown in Fig. 4(b)–(c). Library search results showed the first peak observed in the EGA thermogram, Fig. 2(d) matched with toluene di-isocyanate attributed to the hard segment of PU, Fig. 4(b). Peak 2 as observed in the same EGA thermogram, Fig. 4(c) refers to the soft segment of the PU material and matched with polyethylene glycol in GC–MS library search. These results demonstrated that the PU is a di-isocyanate and polyethylene glycol-based PU.

Mechanical testing

Tensile test

The stress–strain curve of PU sealant is shown in Fig. 4(d). Dimensional details of tensile specimens can be found in SI, Fig. S2. A nonlinear elastic behavior throughout the entire stress–strain curve is observed. Furthermore, it shows a sudden drop indicating rupture. Failure occurs in a purely elastic manner. The elongation at break was at 709.6%, with tensile stress at the break at 331 Psi or about 2.2 MPa only. This could be attributed to fillers, plasticizers, etc., added to the PU base affecting tensile strength and elongation.

Compression–deflection

The 10% and 30% compression–deflection test results are shown in Fig. S3(a). It follows the ASTM D575-91 standard; details can be found in SI with dimensions shown in Fig. S3(b). For both 10% and 30% deflection, PU experienced low compressive stress of 0.08 and 0.33 MPa, respectively. From Fig. S3(c), at 10% compression, there was no plastic deformation observed. This may be due to the low crosslink density and strong filler-to-polymer matrix bonding. However, at a relatively higher compressive stress of 30%, it was only plastically deformed 1.2%, most likely due to a tear in the matrix or matrix to the filler surface caused by compression shear stress.

Durometer hardness

The shore hardness value measures the material's resistance to indentation. There are different shore hardness scales for measuring the hardness of various materials, i.e., soft rubbers and rigid plastics. Shore, A hardness value of PU sealant is estimated at a little above 40, which puts it under medium soft. With this low hardness scale value, it can be assumed that the chain extender is not used extensively.

Electrical testing

Dielectric constant

The dielectric constant measures the electric potential energy by subjecting the material to an electric field that induces polarization.[26] It is the ratio of the dielectric permittivity against a vacuum or dry air. A relatively low dielectric constant will prevent heating the matrix when exposed to a high electric field. The calculated average dielectric constant of PU is 4.8 at 5 Hz, 1 V.
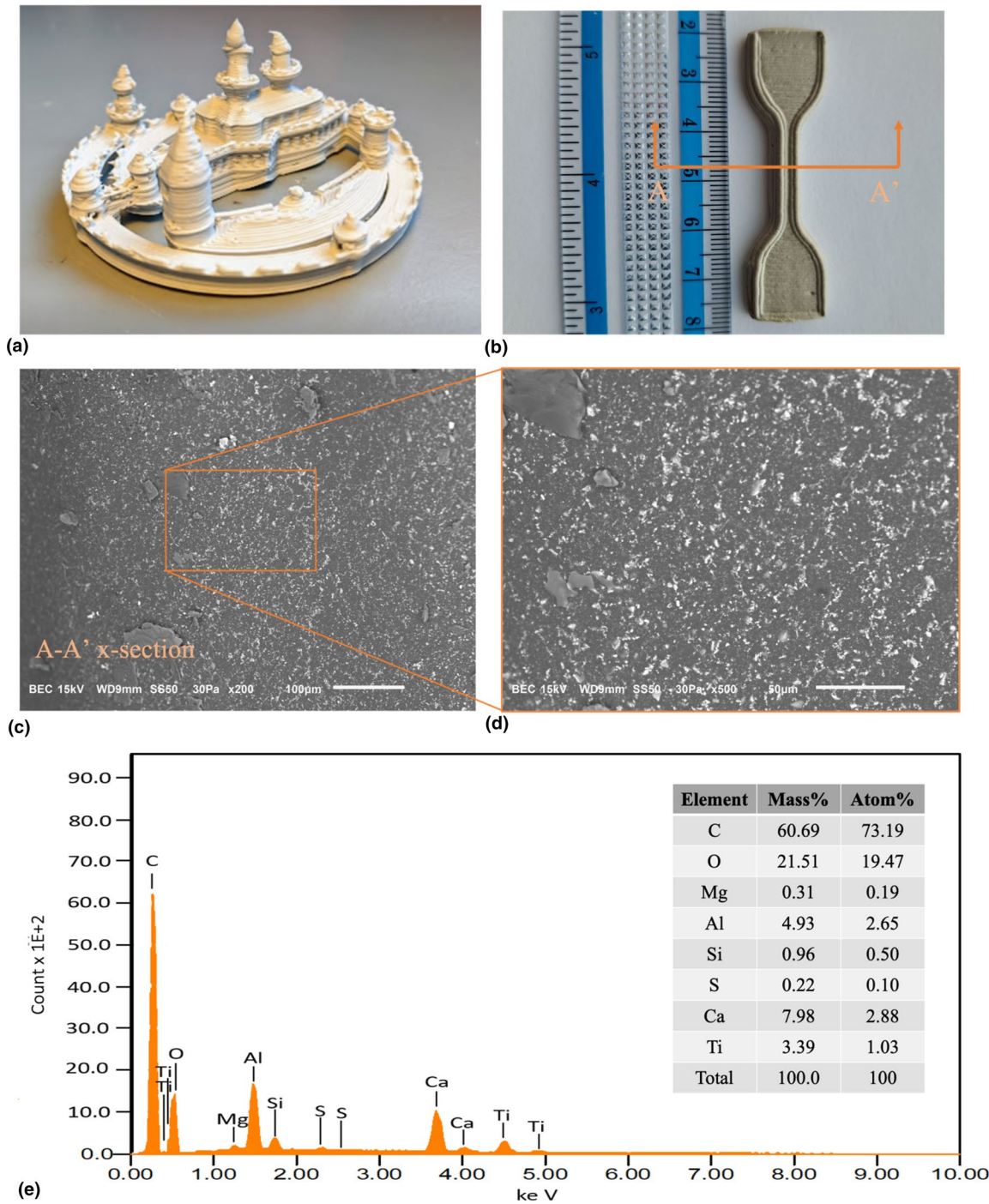
Figure 3. (a) DIW of polyurethane sealant, (b) macro and SEM images for polyurethane BEC images at ×100 (c) and ×1000 (d) magnifications, and (e) EDS spectra of image (d) showing its elemental composition.

Thermal conductivity

Thermal conductivity is a measure that reflects how easily heat flows through a material.[27] A steady-state technique measures the conductivity. If a known amount of heat per unit time P flows through the sample, then for a given geometry, the conductivity can be calculated by measuring the temperature difference created across the sample. The calculated thermal conductivity is 0.2184 W/m K.
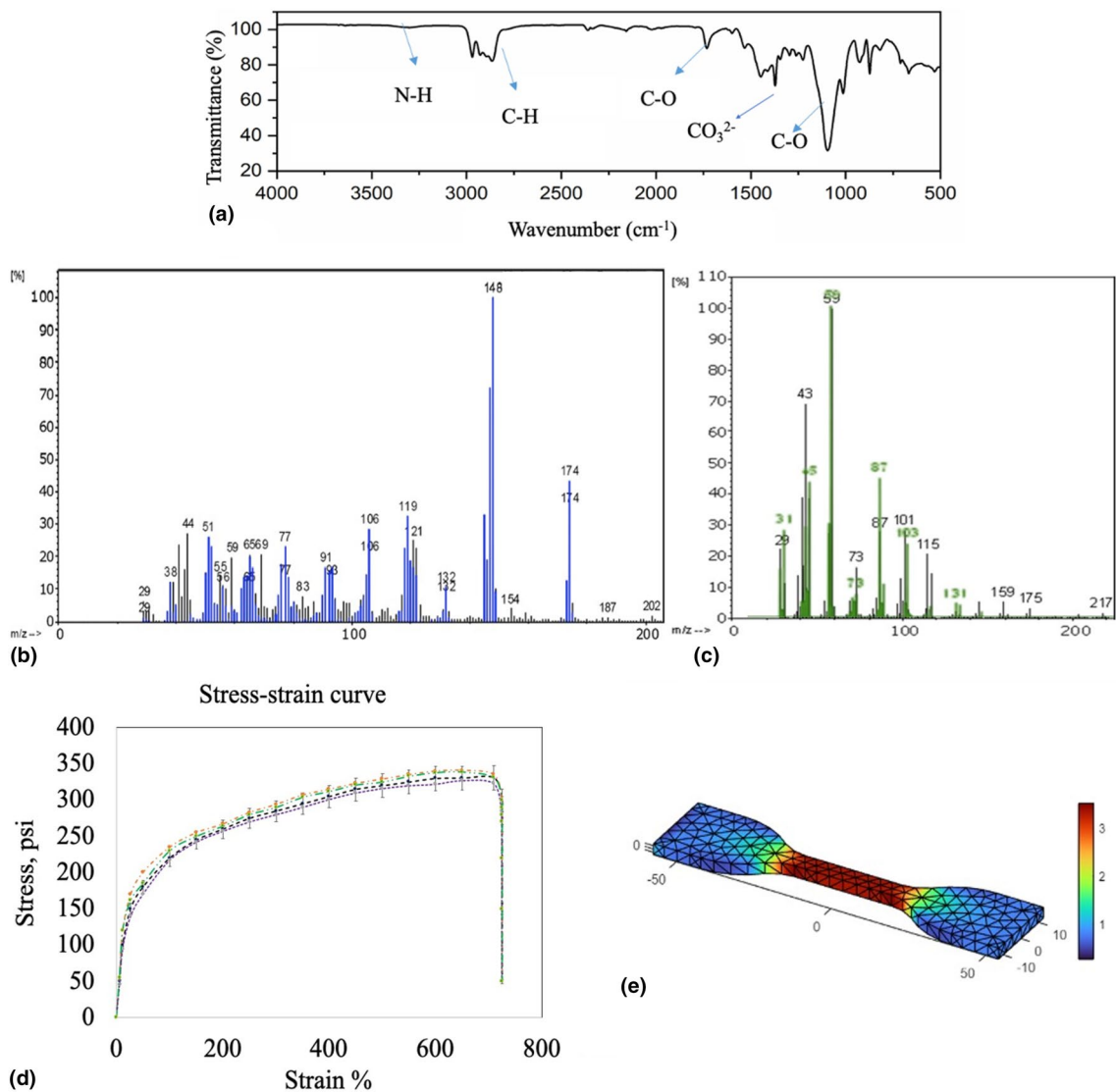
Figure 4. (a) FTIR and GC–MS spectra of polyurethane sealant showing identification of (b) TDI for 1st-peak EGA and (c) polyethylene glycol for 2nd peak of EGA, (d) stress–strain curve for 3D-printed polyurethane sealant, and (e) MATLAB generated finite element analysis of tensile bar image showing stresses at various parts of 3D-printed polyurethane.

Finite element analysis and future work

Finite element analysis (FEA) uses mathematical language in partial derivative equations as a numerical solution to engineering problems.[28] A structure is divided into portions of finite elements (FEs) by splitting its spatial domain via a meshing procedure. It is a highly effective technique that allows validation designs even before a physical prototype is made.[29] FEA is a more robust method to validate initial designs than proceeding directly to physical testing, which can otherwise be expensive. It is also straightforward to adjust an FEA model such that failures can be avoided and can be easily spotted early on.

Shown in Fig. 4(e) is the FE simulation generated from an image fitted based on the values from empirical or experimental data. MATLAB code can be found in the SI. Important PU properties used in the code include Young's modulus = 331 Psi, Poisson's ratio = 0.39, density = 1.76 g/cm^3, etc. Modeled like a load/displacement problem, FEA simulation proceeds when a tensile load is applied, and fracture is observed along the length of the specimen.[30] One end of the specimen model is fixed from the usual tensile testing under uniaxial loading, and load/displacement is applied from another end. The 3D-printed PU used for the FDM model is assumed to be homogeneous and isotropic. Acceptable stress values are calculated throughout the image, and maximum stress concentration can be found in the midsection. However, this FE simulation needs further validation. This can be done by further mesh analysis (i.e., finer mesh size improves accuracy but demands higher computational resources[30] and grid independence studies). This will be part of the future work on 3D printing of PUs.

Conclusion

This study demonstrated that a readily and commercially available PU sealant could be a cost-effective ink for DIW 3D printing. Based on tests conducted in this work, we have identified the sealant as isocyanate NCO-terminated quasi-prepolymers with PU. It is made by reacting isocyanate-terminated PU prepolymer with moisture and forms urea groups. The reaction forms a carbamic acid intermediate that dissociates to carbon dioxide. An amine further reacts with other NCO groups to form urea linkages. When the polymer emerges from the cartridge and is exposed to moisture, its curing and polymerization spontaneously occur. This made the PU very easy to 3D print via DIW. Rheological characterization shows shear-thinning behavior critical for successful DIW 3D printing. The oscillatory experiment indicates a viscoelastic behavior, which is elastic at low strains and plasticity above a crucial shear strain. The storage modulus (G') of 8 kPa obtained is sufficient to print rigid structures without filament sagging. FTIR shows little to no C=O and N=H that is responsible for hydrogen bonds that are responsible for additional strength in the polymer matrix; sealant reformation during elongation, and bond with a plasticizer that has a C=O or carbonyl group in its chain structure.

Furthermore, mechanical test results of printed structures showed standard sealant properties when cured: high-performance sealant with high elongation and low modulus. Future work should address the control and match of the full curing time or hardening time based on the catalyst and accelerant chemistries for PU (organo-lead compounds, piperazines, or trialkyl amines) or the use of controlled moisture and temperature conditions. For further synergistic additives for increased application functionality, we can utilize nanomaterials. This may include studies involving modifications incorporating carbon nanotubes (CNT), graphene oxide (GO), or its combination thereof for improved electrical and thermal conductivity and increased mechanical properties.

Acknowledgements

Declarations

Conflict of interest

There are no conflicts of interest to declare.

Supplementary Information

The online version contains supplementary material available at https://doi.org/10.1557/s43579-023-00407-5.

References

1. T.D. Ngo, A. Kashani, G. Imbalzano, K.T.Q. Nguyen, D. Hui, Additive manufacturing (3D printing): a review of materials, methods, applications, and challenges. Composites B **143**, 172–196 (2018)
2. G.M. Elahee, L.-H. Rong, C. Breting, J. Bonilla-Cruz, T.E. Ceniceros, Z.J. Smith, J. Ge, X. Cheng, M. Xu, M. Yang, E.L. Ribeiro, E.B. Caldona, R.C. Advincula, Acrylic sealants as practicable direct ink writing (DIW) 3D-printable materials. MRS Commun. **13**, 299–305 (2023)
3. P. Chung, J.A. Heller, M. Etemadi, P.E. Ottoson, J.A. Liu, L. Rand, S. Roy, Rapid and low-cost prototyping of medical devices using 3D printed molds for liquid injection molding. J. Vis. Exp. **88**, e51745 (2014). https://doi.org/10.3791/51745
4. M. Moczadlo, Q. Chen, X. Cheng et al., On the 3D printing of polypropylene and post-processing optimization of thermomechanical properties. MRS Commun. **13**, 169–176 (2023)
5. R.C. Advincula, J.R.C. Dizon, E.B. Caldona, R.A. Viers, F.D.C. Siacor, R.D. Maalihan, A.H. Espera Jr., On the progress of 3D-printed hydrogels for tissue engineering. MRS Commun. **11**, 539 (2021)
6. D.B. Gutierrez, E.B. Caldona, R.D. Espiritu, R.C. Advincula, The potential of additively manufactured membranes for selective separation and capture of CO_2. MRS Commun. **11**, 391 (2021)
7. R.C. Advincula, J.R.C. Dizon, Q. Chen, I. Niu, J. Chung, L. Kilpatrick, R. Newman, Additive manufacturing for COVID-19: devices, materials, prospects, and challenges. MRS Commun. **10**(3), 413 (2020)
8. E.B. Caldona, J.R.C. Dizon, R.A. Viers, V.J. Garcia, Z.J. Smith, R.C. Advincula, Additively manufactured high-performance polymeric materials and their potential use in the oil and gas industry. MRS Commun. **11**, 701 (2021)
9. A.D. Valino, J.R.C. Dizon, A.H. Espera Jr., Q. Chen, J. Messman, R.C. Advincula, Advances in 3D printing of thermoplastic polymer composites and nanocomposites. Prog. Polym. Sci. **98**, 101162 (2019)
10. Z.J. Smith, D.R. Barsoum, Z.L. Arwood, D. Penumadu, R.C. Advincula, Characterization of micro-sandwich structures via direct ink writing epoxy based cores. J. Sandw. Struct. Mater. **25**(1), 112–127 (2022)
11. J.A. Lewis, J.E. Smay, J. Stuecker, J. Cesarano, Direct ink writing of three-dimensional ceramic structures. J. Am. Ceram. Soc. **89**, 3599–3609 (2006). https://doi.org/10.1111/j.1551-2916.2006.01382.x
12. J.A. Lewis, Direct ink writing of 3D functional materials. Adv. Funct. Mater. **16**(17), 2193–2204 (2006)
13. H.-W. Engels, H.-G. Pirkl, R. Albers, R.W. Albach, J. Krause, A. Hoffmann, H. Casselmann, J. Dormish, Polyurethanes: versatile materials and sustainable problem solvers for today's challenges. Angew. Chem. Int. Ed. **52**(36), 9422–9441 (2013)
14. T.M. Crescentini et al., Mass spectrometry of polyurethanes. Polymer **181**, 121624 (2019). https://doi.org/10.1016/j.polymer.2019.121624
15. A.L. Daniel da Silva, J.M. Martín-Martínez, J.C. Bordado, Influence of the free isocyanate content in the adhesive properties of reactive trifunctional polyether urethane quasi-prepolymers. Int. J. Adhes. Adhes. **26**(5), 355–362 (2006). https://doi.org/10.1016/j.ijadhadh.2005.06.001
16. Zafar, F., Chapter 1 polyurethane. In: *Polyurethane: An Introduction* (IntechOpen, London, 2012). https://doi.org/10.5772/51663
17. J.N. Hahladakis et al., An overview of chemical additives present in plastics: migration, release, fate and environmental impact during their use, disposal and recycling. J. Hazard. Mater. **344**, 179–199 (2018). https://doi.org/10.1016/j.jhazmat.2017.10.014
18. LOCTITE® PL Concrete, Non-sag Polyurethane Sealant Page 1 of 4 Technical Data Sheet. https://dm.henkel-dam.com/is/content/henkel/tds-us-loctite-loc-pl-concrete-non-sag-polyurethane-sealant-2020-09-01. Accessed 22 March 2023
19. M.T. Espino, B.J. Tuazon, A.H. Espera et al., Statistical methods for design and testing of 3D-printed polymers. MRS Commun. (2023). https://doi.org/10.1557/s43579-023-00332-7
20. Admin (no date) Engine SR—standard resolution 3D printer, Hyrel 3D. http://www.hyrel3d.com/portfolio/engine-sr-standard-resolution/. Accessed 27 Jan 2023
21. A.H. Espera, J.R.C. Dizon, A.D. Valino et al., On the 3D printability of silicone-based adhesives via viscous paste extrusion. MRS Commun. **13**, 102–110 (2023)

22. X.-D. Chen, N.-Q. Zhou, H. Zhang, Preparation and properties of cast polyurethane elastomers with molecularly uniform hard segments based on 2, 4-toluene diisocyanate and 3, 5-dimethyl thio toluene diamine. J. Biomed. Sci. Eng. **2**, 245–253 (2009)

23. G. Lligadas, J.C. Ronda, M. Galià, U. Biermann, J.O. Metzger, Synthesis and characterization of polyurethanes from epoxidized methyl oleate based polyether polyols as renewable resources. J. Polym. Sci. A **44**, 634–645 (2006)

24. X. Feng, S. Yusheng, H. Shuhuai, Synthesis and performance of transparent casting polyurethane resin. J. Wuhan Univ. Technol. Mater. Sci. Ed. **20**, 24–28 (2005)

25. J.R. Saunders, The reactions of isocyanates and isocyanate derivatives at elevated temperatures. Rubber Chem. Technol. **32**, 337 (1959)

26. C.L. Cao, J. Cheng, X.D. Liu, R. Wang, J.Y. Zhang, J. Qu, U. Jaeger, Study of properties of one-component moisture-curable polyurethane and silane modified polyurethane adhesives. J. Adhes. Sci. Technol. **26**(10–11), 1395–1405 (2012)

27. X. Wei, T. Luo, Chain length effect on thermal transport in amorphous polymers and a structure–thermal conductivity relation. Phys. Chem. Chem. Phys. **21**(28), 15523–15530 (2019). https://doi.org/10.1039/C9CP02397F

28. D. Yang, M. Tian, Y. Dong, H. Liu, Y. Yu, L. Zhang, Disclosed dielectric and electromechanical properties of hydrogenated nitrile–butadiene dielectric elastomer. Smart Mater. Struct. **21**(3), 035017 (2012). https://doi.org/10.1088/0964-1726/21/3/035017

29. C.S. Miron-Borzan, E. Sabau, M. Mera, P. Berce, Research regarding the manufacturing through AM technologies of an implant for cervical disc replacement. MATEC Web Conf. **137**, 02008 (2017)

30. D.G. Puttaraju, H.G. Hanumantharaju, Finite element analysis and validation of tensile properties of carbon fiber reinforced polymer matrix composites. Mater. Today: Proc. **62**, 2800–2807 (2022)